ACS OMEGA

Open Access

http://pubs.acs.org/journal/acsodf

Article

Fabrication of an Adhesive Small Intestinal Submucosa Acellular Matrix Hydrogel for Accelerating Diabetic Wound Healing

Yao Chen,[⊥] Miner Hu,[⊥] Honghua Hu,[⊥] Shunxian Ji, Leyi Huang, Wei Wei,* Kun Zhao,* and Chong Teng*

Cite This: *ACS Omega* 2023, 8, 46653−46662

Read Online

ACCESS | Metrics & More | Article Recommendations

ABSTRACT: The treatment of diabetic skin defects comes with enormous challenges in the clinic due to the disordered metabolic microenvironment. In this study, we therefore designed a novel composite hydrogel (SISAM@HN) with bioactive factors and tissue adhesive properties for accelerating chronic diabetic wound healing. Hyaluronic acid (HA) modified by *N*-(2-aminoethyl)-4-(4-(hydroxymethyl)-2-methoxy-5-nitrosophenoxy) butanamide (NB) held the phototriggering tissue adhesive capacity. Decellularized small intestinal submucosa (SIS) was degreased and digested to form the acellular matrix, which facilitated bioactive factor release. The results of the burst pressure test demonstrated that the *in situ* formed hydrogel possessed a tissue adhesive property. *In vitro* experiments, based on bone marrow stromal cells, revealed that the SIS acellular matrix-containing hydrogel contributed to promoting cell proliferation. *In vivo*, a diabetic mouse model was created and used to evaluate the tissue regeneration function of the obtained hydrogel, and our results showed that the synthesized hydrogel could assist collagen deposition, attenuate inflammation, and foster vascular growth during the wound healing process. Overall, the SIS acellular matrix-containing HA hydrogel was able to adhere to the wound sites, promote cell proliferation, and facilitate angiogenesis, which would be a promising biomaterial for wound dressing in clinical therapy of diabetic skin defects.

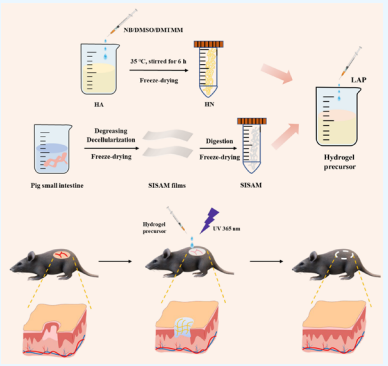

1. INTRODUCTION

Diabetes mellitus (DM) is a common but serious metabolic disorder.[1,2] With the increasing number of cumulative cases, DM has been a severe disease that endangers human beings.[3] Diabetic ulcer, a common complication of diabetes, characterized by the difficulty of wound healing and the high incidence of amputation and mortality, has brought heavy mental and physical pressure on patients and also a huge economic burden on society.[4] The well-known therapeutic strategies for diabetic wound healing involve blood glucose regulation, wound debridement, revascularization, wound decompression, and wound dressing.[5] Among these therapeutic regimens, wound dressing is applied widely in the clinic owing to the isolation from an external environment and the delivery of medicine to wound sites directly.[6] Multiple kinds of wound dressings have been developed for accelerating diabetic wound healing, like biocompatible membranes,[7] electrospun fibers,[8] and functional hydrogels.[9] Among the candidates, hydrogels have attracted much more attention due to the unique features including biocompatibility, porous structure, absorption of excess tissue exudate, and facilitation of therapeutic factor delivery.[10,11]

Hydrogels combined with natural macromolecular polymers like gelatin,[12] chitosan,[13] silk fibroin,[14] and hyaluronic acid (HA)[15] have aroused interests all over the world. HA, a multifunctional substrate present in the human body, is considered as one of the most potential repair materials for skin tissues.[16−19] The content and metabolism of HA affect the process of skin maturation and aging. Moreover, HA could enhance transdermal absorption and maintain skin moist.[20,21] There have been numerous research studies concentrated on HA for tissue repair. For example, Li et al. have explored self-healing HA hydrogels based on dynamic Schiff base linkages as biomaterials.[22] Zhao et al. have developed double cross-linked biomimetic HA-based hydrogels with thermo-stimulated self-contraction and tissue adhesiveness for accelerating postwound closure and wound healing.[23] However, HA cannot be gelatinized itself.[24] Previous researches reported that *o*-nitrobenzene (NB) was modified onto an HA molecule chain to obtain a phototriggered macromolecule HANB (HN);[25] furthermore, NB modification made it possible for hydrogel to connect to the skin tissue through a Schiff-base reaction.[26]

Received: August 3, 2023
Revised: November 10, 2023
Accepted: November 14, 2023
Published: November 29, 2023

The extracellular matrix (ECM) plays a crucial role in constructing a physical extracellular environment, signal transduction, and cell migration.[27] Recently, abundant research for the application of the ECM in the field of injured tissue repair has been published. For example, Wang et al. have developed exosome-laden self-healing injectable hydrogels to enhance diabetic wound healing.[28] Zhang et al. have explored exosome/metformin-loaded self-healing conductive hydrogels to rescue microvascular dysfunction and promote chronic diabetic wound healing by inhibiting mitochondrial fission.[29] Small intestinal submucosa (SIS) is a natural ECM, which contains numerous fibronectin, laminin, collagens, especially collagen types I and III, and multiple growth factors, such as the transforming growth factor-β (TGF-β), vascular endothelial growth factor (VEGF), and basic fibroblast growth factor (bFGF).[30,31] The small intestinal submucosa acellular matrix (SISAM) is decellularized SIS that maintains the structural and molecular components while the cellular content is removed.[32] So far, accumulated evidence has shown that the SISAM exhibits enormous potential in biological scaffolds, surgical meshes, cell culturing, and wound dressing because of the preeminent biocompatibility and bioactivity.[33] However, the clinical strategies are still limited due to complicated delivery systems and potential side effects.[34]

Herein, we design and fabricate a multifunctional bioactive hydrogel (SISAM@HN) for accelerating diabetic wound healing. In the present study, HA is modified with NB, and SIS is decellularized, degreased, and digested for releasing the SISAM. This combination integrates the advantages of both HN and SIS that synergistically adhere to tissues and promote tissue regeneration. To the best of our knowledge, HN and SIS have not been used together for diabetic wound dressing before. In this study, HN is characterized by ^{1}H NMR, and the composite hydrogel is characterized by SEM. The adhesion and swelling kinetics are also studied. An *in vitro* biocompatibility experiment is conducted, and the therapeutic effect of diabetic skin defects *in vivo* is explored.

2. MATERIALS AND METHODS

2.1. Materials. Hyaluronic acid (HA), 4-(4,6-dimethoxy-1,3,5-triazin-2-yl)-4-methylmorpholinium chloride (DMTMM), dimethyl sulfoxide (DMSO), 2-(*N*-morpholino)-ethanesulfonic acid monohydrate (MES), sodium chloride (NaCl), Triton X-100, aqueous ammonia ($NH_3{\cdot}H_2O$), methanol (CH_3OH), chloroform ($CHCl_3$), ethanol (C_2H_5OH), and pepsin were brought from Aladdin (Shanghai, China). *N*-(2-Aminoethyl)-4-(4-(hydroxymethyl)-2-methoxy-5-nitrosophenoxy) butanamide (NB) and lithium phenyl-2,4,6-trimethylbenzoyl phosphinate (LAP) were supplied by Haining Jurassic Biotech Company Ltd. Cell counting kit-8 (CCK-8) was obtained from Beyotime (Shanghai, China). Recombinant human basic fibroblast growth factor gel (rhbFGF, SL Pharm) was used.

2.2. Synthesis of HN. HA (2 g) was dissolved in 100 mL of MES solution (pH 5.3) at 35 °C. Then, 60 mg of NB was dissolved in 10 mL of dimethyl sulfoxide (DMSO) and was introduced into the solution. Next, 1.2 g of DMTMM was added into the mixture in three batches with an interval of 0.5 h, and the reaction was allowed to last for 3 h. The prepared HA-NB was dialyzed with a NaCl solution (0.1M) and freeze-dried for storage.

2.3. Preparation of the Small Intestinal Submucosa Acellular Matrix (SISAM). The SISAM was fabricated through a decellularization and degreasing process. In brief, the fresh pig small intestine was washed and soaked repeatedly with plenty of deionized water until the mucosal layer and sarcoplasmic layer were edema. Then, the mucosal layer and sarcoplasmic layer were scraped away, and milky white, translucent, flexible small intestinal submucosa (SIS) was obtained. SIS was immersed in decellularized solution (10 mL of Triton X-100 and 1 mL of $NH_3{\cdot}H_2O$ dissolved in 1000 mL of deionized water) at 4 °C for 72 h, and SIS was soaked in $CH_3OH/CHCl_3$ (1:1) for 24 h to degrease. Subsequently, SIS was stirred in C_2H_5OH for 48 h for $CH_3OH/CHCl_3$ degreaser removal. Finally, the obtained SISAM films were stored at 4 °C after lyophilization. To promote the release of bioactive factors more efficiently, SISAM films were digested by pepsin. One hundred mg of SISAM films and 100 mg of pepsin were added into 10 mL of acidic aqueous solution (pH 1) and stirred at 37 °C for 3 h. The mixture was titrated to neutral with NaOH for pepsin inactivation, and the SISAM was stored in −40 °C after lyophilization.

2.4. Fabrication of the Composite Hydrogel (SISAM@HN). HN, SISAM, and the photoinitiator (LAP) were dissolved in deionized water at final concentrations of 2, 1, and 0.025%, respectively. The hydrogel precursor was dropped into a preprepared PDMS mold (Φ 10 mm × 2 mm) and irradiated under 365 nm UV light for 20 s for photocuring.

2.5. Characterization. The microstructure of the hydrogel was exhibited by scanning electron microscopy (SEM, ZEISS SIGMA 500). ^{1}H Nuclear magnetic resonance (^{1}H NMR) spectra of HN were analyzed by an NMR spectrometer (Bruker, 400 MHz).

2.6. Swelling Kinetic Studies. The weights of lyophilized hydrogels were recorded as m_0, and a swelling kinetic experiment was conducted by weighting the hydrogels immersed in PBS at a required time (m_t). The swelling ratio was calculated as follows:

$$\text{swelling ratio} = \frac{m_t}{m_0} \times 100\% \quad (1)$$

2.7. Burst Pressure Test. The adhesive capability of the hydrogels was tested according to a modified ASTM standard (F2392-04) using a custom-made burst pressure apparatus.[35,36] Briefly, a collagen sausage casing was used as a tissue model and fixed in the apparatus. A hole was created in the middle of the collagen sausage casing with a syringe needle (18G). Hydrogel precursors (200 μL) were applied to the hole, and UV irradiation (365 nm, 100 mW/cm^2, 20 s) was used to cure the hydrogel. Finally, pressure was made from pumping saline continuously. The pressures at failure were recorded ($n \geq 3$).

2.8. Compressive Test. We conducted compressive tests of hydrogels (Φ 10 × 2 mm) under an electronic testing machine (MTS C41) with a 50 N load cell. The compressive rate was set as 1 mm/min. The compressive modulus was calculated from the linear region of the stress−strain curve.

2.9. Cell Viability and Proliferation. Rat BMSCs were obtained and used as our previous study.[6] Hydrogel extract was prepared by immersing hydrogels (10 mm in diameter, 2 mm in height) in 10 mL of Dulbecco's modified Eagle's medium (DMEM, containing a 10% fetal bovine serum and 1% penicillin−streptomycin mixture) for 24 h. The extract was sterilized with a 0.22 μm filter. BMSCs were cultured with the extract at 37 °C and 5% CO_2. Normal DMEM was used as a control group. Cell viability was determined by a Live/Dead assay and observed with an inverted fluorescence microscope.

https://doi.org/10.1021/acsomega.3c05682
ACS Omega 2023, 8, 46653−46662

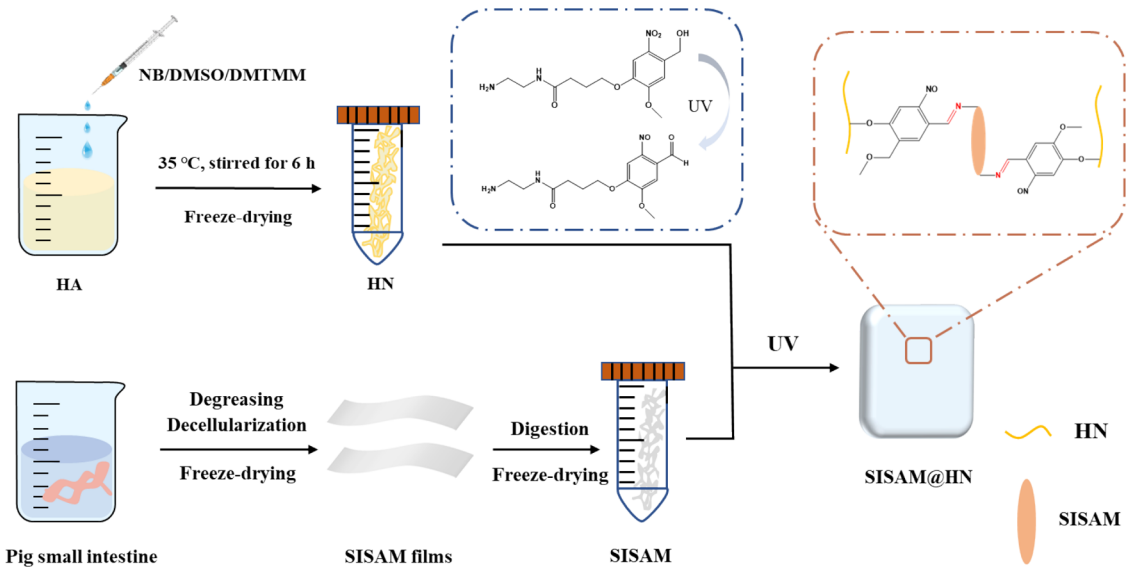

Figure 1. Schematic illustration of the SISAM@HN hydrogel.

The proliferation was studied by a CCK-8 assay, and the optical density (OD) value was obtained by a microplate reader.

2.10. Diabetic Mouse Model. A diabetic mouse model was created according to previous studies.[37,38] All animal procedures were performed according to the standard guidelines approved by the Zhejiang University Ethics Committee (Ethical No. ZJU20220190). C57BL/6 mice (20−25 g, six-weeks-old, male) were obtained from Hangzhou Paisiao Biotechnical Ltd. and bred for adaptation with no dietary restrictions under the standard laboratory environment conditions, including a temperature of 22 ± 2 °C, a humidity of 40−60%, and a 12 h light/dark cycle, for 1 week. Diabetes was induced by a once daily intraperitoneal injection of streptozotocin (STZ, Sigma-Aldrich, 55 mg/kg) in sodium citrate buffer (pH 4.3) for five consecutive days. Two weeks after the STZ injection, the diabetic state was confirmed by blood glucose above 16.6 mmol/L.

2.11. Cutaneous Wound Preparation and Measurement. The diabetic mice were anesthetized with 1% pentobarbital sodium. After hair removal and sterilization of the surgical sites, the full-thickness cutaneous wounds were induced by a sterile biopsy punch (10 mm in diameter) and scalpels. The diabetic mice were divided into three groups (n = 15): (1) control (PBS), (2) rhbFGF, and (3) hydrogel (SISAM@HN). The mice in three groups received the corresponding treatments, and the wound sites were dressed with sterile gauze.

The cutaneous wounds were photographed and measured at four time points (0, 3, 7, and 14 days). Wound areas were analyzed by ImageJ software (NIH, Bethesda, MD, USA).

2.12. Histological Analysis. Wound tissues of mice (n = 5, per group, per time points) from three groups were excised at three time points (3, 7, and 14 days). After fixing in paraformaldehyde for 24 h and embedding in paraffin, the sections (4 μm) were stained with hematoxylin and eosin (H&E) using standard protocols. The stained sections were photographed digitally and viewed by a digital slide scanner (KFBIO, Ningbo). Masson's trichrome staining was also performed on paraffin sections according to the standard protocols, and the stained sections were analyzed for collagen volume fraction (%) by ImageJ software (NIH, Bethesda, MD, USA).

2.13. Immunohistochemistry and Immunofluorescence. The sections were treated with heat-induced antigen recovery and the removal of endogenous peroxidase activity. After BSA blocking, the sections were incubated with specific primary antibodies (rabbit anti-CD31, Zhongshan; rabbit anti-TNFA, Proteintech; rabbit anti-VEGFA, Proteintech) overnight at 4 °C. On the next day, the sections were incubated with the secondary antibody (goat antirabbit) conjugated with HRP for immunohistochemistry or with CoraLite594 for immunofluorescence. The nucleus was stained by hematoxylin and 4′,6-diamidino-2-phenylindole (DAPI) for immunohistochemistry and immunofluorescence, respectively. The stained sections were photographed digitally and viewed by a disital slide scanner (KFBIO, Ningbo).

2.14. Statistical Analysis. Statistical analysis was performed with GraphPad Prism software version 9 (GraphPad Software, La Jolla, USA). All values were presented as means ± SD. Comparisons between two groups were completed by using Student's t-test. Data for multiple comparisons were analyzed by using one-way analysis of variance (ANOVA). *p < 0.05, **p < 0.01, ***p < 0.001, and ****p < 0.0001 were considered to be statistically significant.

3. RESULTS AND DISCUSSION

The phototriggering cross-linked and tissue adhesive SISAM@HN hydrogel was fabricated according to the schematic as shown in Figure 1. NB was modified onto an HA molecule chain by DMTMM-assisted esterification between amino groups in NB and carboxyl groups in HA. The conversion of methylol groups of NB to aldehyde groups under UV irradiation prompted the cross-linking of synthesized HN-SISAM aqueous solution, owing to the Schiff-base reaction between aldehyde groups and amino groups of the SISAM.[26] Significantly, not only SISAM amino groups reacted with aldehyde, but also, tissue amino groups did, resulting in the high adhesive capacity to tissues. At the same time, a fresh pig small intestine was transformed to SISAM films after rinsing, degreasing, decellularization, and lyophilization. In order to simplify the biological factors released, the SISAM was

https://doi.org/10.1021/acsomega.3c05682
ACS Omega 2023, 8, 46653−46662

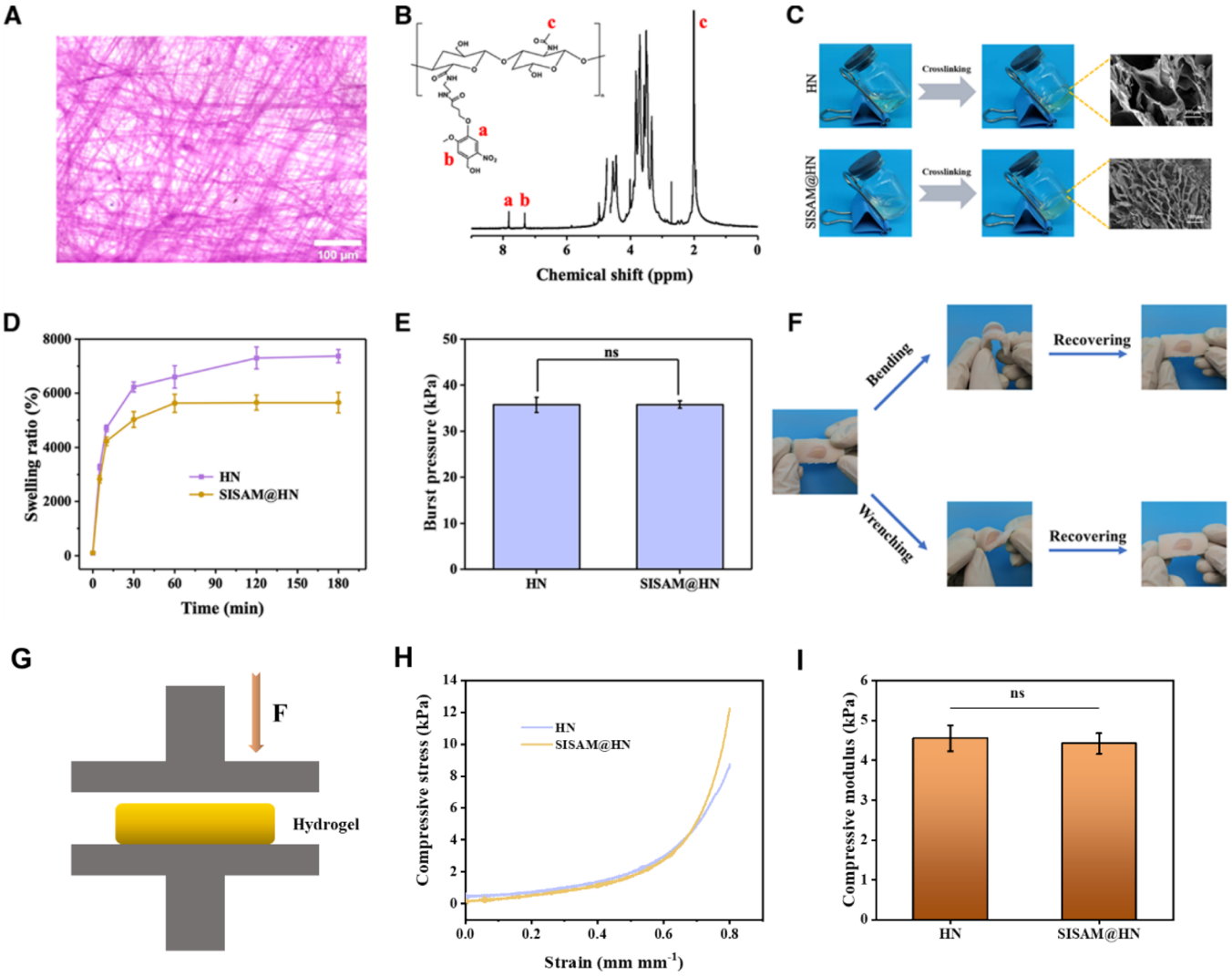

Figure 2. Characterizations of the hydrogels. (A) Histological evaluation of SISAM films, (B) ^{1}H NMR spectrum of the HN macromolecule, (C) digital photos of the curing process of hydrogels and SEM images of the cross sections of hydrogels, (D) swelling kinetics of the HN hydrogel and SISAM@HN hydrogel, (E) burst pressure test results of HN and SISAM@HN hydrogels, and (F) photos of SISAM@HN adhesion on porcine skin *ex vivo* and recovered after bending and wrenching. (G) Schematic diagram of the compressive test. (H) Compressive stress−strain curves. (I) Compressive modulus of hydrogels.

designed to be digested by pepsin. Finally, the SISAM was mixed into the HN precursor and irradiated by 365 nm UV (100 mW/cm^2) for 20 s, and the SISAM@HN composite hydrogel was fabricated.

Characterizations of the Hydrogels. First, as shown in Figure 2A, H&E staining indicated that there was no cell remaining in the prepared SIS films, ensuring the desired acellular matrix in subsequent experiments.[39] On the other side, ^{1}H NMR spectra of HN (Figure 2B) showed peaks at δ = 7.3 ppm and δ = 7.8 ppm, which are ascribed to the hydrogen atoms of NB benzene.[25] It indicated that NB molecules were grafted onto the HA chain, and HN was fabricated successfully. As photocuring hydrogels, HN and SISAM@HN precursors were demonstrated to be cross-linked into hydrogels under 365 nm UV irradiation (100 mW/cm^2, 20 s) (Figure 2C). After lyophilization, SEM was applied to observe the microstructure of the hydrogels. The porous channels existed in the hydrogels, and the porous microstructure ensured the holding of H_2O molecules and the delivery of therapeutic factors. Obviously, there was a filiform-digested SISAM surrounded by the channels, resulting in the decreasing of pore size. Swelling kinetics was studied, and H_2O was absorbed into the network of the hydrogel in 30 min (Figure 2D). This property could be helpful in removing excess tissue exudate and maintaining moisture in defect sites. Interestingly, the SISAM@HN hydrogel exhibited a lower equilibrium swelling ratio than the pure HN hydrogel, suggesting that the SISAM in the precursor facilitated the cross-linking of the hydrogel and formed a denser network. As a wound dressing, the hydrogels were required to adhere to wound sites throughout the wound recovery process. We conducted burst pressure tests to evaluate the adhesive property, and the results showed that the adhesive strengths of HN and SISAM@HN were about 35.73 and 35.78 kPa, respectively (Figure 2E). It indicated that the addition of the SISAM had almost no positive or negative effect on the adhesion of the original HN. The tissue adhesive property guaranteed secure fit to wound in the therapeutic process.[40,41] *Ex vivo*, as displayed in Figure 2F, the SISAM@HN hydrogel formed *in situ* on the porcine skin could recover to its original state after bending and wrenching, suggesting a

https://doi.org/10.1021/acsomega.3c05682
ACS Omega 2023, 8, 46653−46662

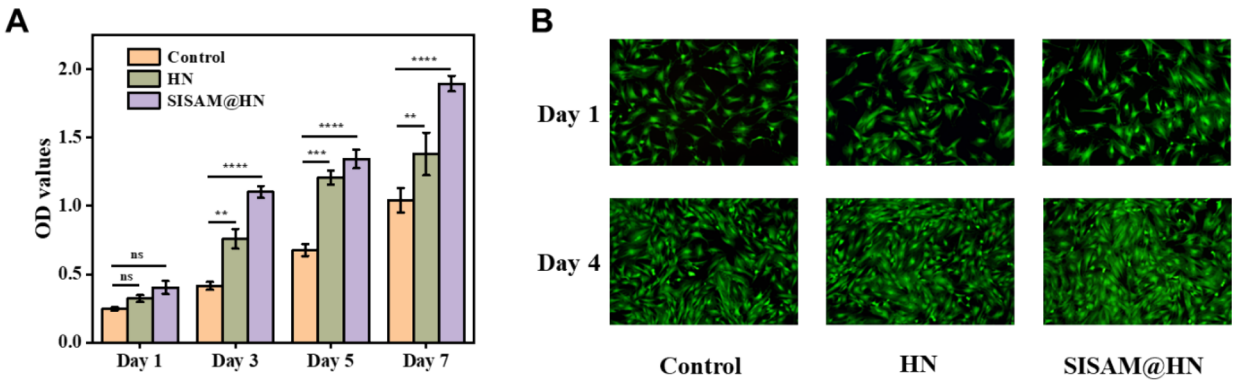

Figure 3. Cytotoxicity of the SISAM@HN hydrogel *in vitro*. (A) Proliferation of BMSCs cultured with hydrogel extract and (B) Live/Dead assay of BMSCs cultured with hydrogel extract on day 1 and day 4.

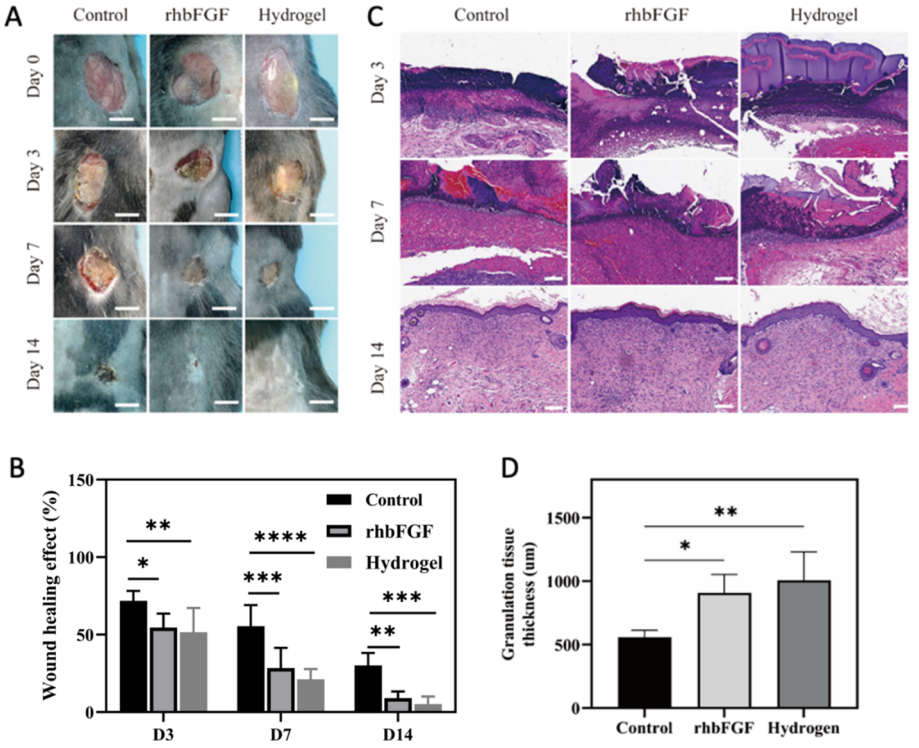

Figure 4. SISAM@HN accelerated diabetic wound healing. (A) Wounds of diabetic mice in all groups at different time points (0, 3, 7, and 14 days). (B) Quantitative analysis of the wound areas ($n = 5$, $^{*}p < 0.05$, $^{**}p < 0.01$). (C) H&E staining of wound sections at day 3, day 7, and day 14. (D) Quantification of the thickness of the granulation tissue at day 14 ($n = 5$, $^{*}p < 0.05$, $^{**}p < 0.01$, $^{***}p < 0.001$).

desirable tissue binding strength and flexibility as a wound dressing. Further, we evaluated the mechanical properties of the hydrogels (Figure 2G). HN and SISAM@HN hydrogels could withstand up to more than 80% strain without fracture (Figure 2H). The compressive moduli of HN and SISAM@HN were about 4.55 and 4.47 kPa (0.3−0.5 mm mm^{-1}) (Figure 2I). These results demonstrated that our prepared hydrogels possessed satisfactory water-absorbing quality, adhesion to skin, and mechanical property, ensuring their potential in the field of skin wound healing.

SISAM@HN Accelerated Cell Proliferation. SISAM@HN was designed as a wound dressing for diabetic skin defects, and the biocompatibility needed to be verified. HN and SISAM@HN were chosen, and the capacity of promoting cell proliferation was investigated. As displayed in Figure 3A, both of HN and SISAM@HN were found to significantly accelerate the proliferation of BMSCs. Especially, the optical density (OD) value of BMSCs cultured with SISAM@HN was significantly higher than that of the control group cultured with a normal cell culture medium on day 7. As a species of the acellular matrix, the SISAM contained numerous biological factors beneficial to cell proliferation, and the biological factors were released easily. In addition, the viability of BMSCs was revealed by a Live/Dead staining assay (Figure 3B). Almost no dead BMSCs (marked by red spots) were observed, and the densities of living BMSCs (marked by green spots) cultured with HN and SISAM@HN were higher than that in the control group. It indicated that as-prepared hydrogels possessed excellent biocompatibility, ensuring application in skin defect repair and tissue regeneration.

SISAM@HN Accelerated Diabetic Wound Healing. In order to evaluate the impact of SISAM@HN on the full-thickness skin wound healing, diabetic mice were divided into three groups: (1) the control group, (2) rhbFGF-treated

https://doi.org/10.1021/acsomega.3c05682
ACS Omega 2023, 8, 46653−46662

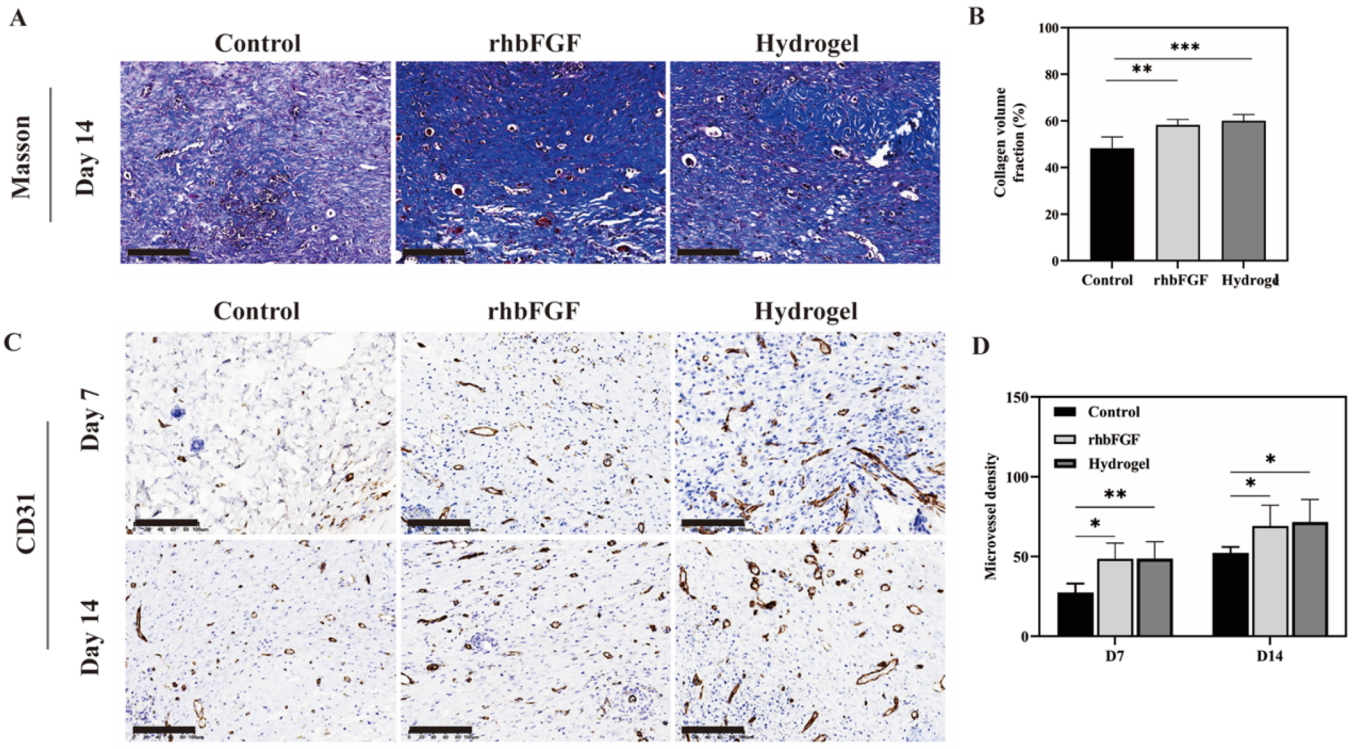

Figure 5. SISAM@HN promoted collagen deposition and vascular growth. (A) Masson's trichrome staining of the wound sections at day 14 (scale bar: 100 μm). (B) Statistical analysis of collagen volume fractions at day 14 (n = 5, $^{**}p < 0.01$, $^{***}p < 0.001$). (C) Immunohistochemistry staining of CD31 expression in the wound sites at day 7 and day 14 (scale bar: 100 μm). (D) Statistical analysis of the amounts of CD31-positive cells per view for neovascularization at day 7 (n = 5, $^{*}p < 0.05$, $^{**}p < 0.01$) and day 14 (n = 5, $^{*}p < 0.05$).

group, and (3) hydrogel (SISAM@HN). Recombinant human basic fibroblast growth factor gel (rhbFGF) is a clinically used drug for diabetic wound treatment and was used as a positive control in this study. Our results showed the gradual improvement of the cutaneous wound in all groups at three specific time points (3, 7, and 14 days), while obviously, the rhbFGF-treated group and the SISAM@HN-treated group facilitated the wound closure in a greater degree compared with the control group (Figure 4A). Quantification of the wound area is displayed in Figure 4B, and at day 14, the wound area was 0.221 ± 0.067 cm^2 in the control group, 0.064 ± 0.027 cm^2 in the rhbFGF-treated group, and 0.041 ± 0.041 cm^2 in the SISAM@HN-treated group, indicating that SISAM@HN not only gained a similar therapeutic efficacy to rhbFGF but also a significant advantage over the control group. To further observe the skin tissue repair under different treatments, H&E staining was applied for complete histological analysis of the cutaneous wound sections. With the increase in healing time, as well as rhbFGF, SISAM@HN achieved accelerated re-epithelialization and well-formed dermal reorganization, including a few new hair follicles. However, the control group had less organized epidermal and dermal reconstructions (Figure 4C). Additionally, it was shown in the quantitative analysis of the granulation tissue thickness that at day 14 (Figure 4D), the SISAM@HN group was nearly twice as thick as the control group but had no significant difference with the rhbFGF-treated group, which demonstrated that SISAM@HN contributed to the formation of the granulation tissue in the diabetic wound healing.

SISAM@HN Promoted Collagen Deposition, Attenuated Inflammation, and Fostered Vascular Growth. Abundant collagen formation played a crucial role in the process of diabetic wound healing.[42] Masson's trichrome staining was performed to analyze collagen deposition in the wound sections, which exhibited that by comparison with the control group, there were more dense and organized collagen fibers in the rhbFGF-treated group and the SISAM@HN-treated group (Figure 5A). Meanwhile, the quantitative evaluation of the collagen volume fraction in Figure 5B showed that the contents of newly formed collagen in the rhbFGF-treated group (58.27 ± 2.38%) and the SISAM@HN-treated group (60.05 ± 2.72%) were significantly higher than that of the control group (48.23 ± 4.92%), which demonstrated that SISAM@HN induced collagen deposition.[43] In addition, the appearance of neovascularization provided nutrients, oxygen, cytokines, and chemokines to ensure the wound healing microenvironment.[44] CD31, a well-established marker for endothelial cells,[45,46] was applied for immunohistochemistry staining. Our results revealed that SISAM@HN and rhbFGF both significantly augmented the amounts of CD31-positive endothelial cells and had microvessel densities higher than that of the control group at day 7 (Figure 5C,D). Furthermore, there were similar changing trends to day 14, suggesting that SISAM@HN simulated angiogenesis in diabetic wound healing.

To further evaluate the ability of SISAM@HN in regulating the wound healing at an early stage, tumor necrosis factor-α (TNF-α, proinflammatory factors) and vascular endothelial growth factor A (VEGFA) in the wound at seventh day postsurgery were stained and investigated. As shown in Figure 6A,B, significantly less expression of TNF-α (red spots) was observed in the SISAM@HN-treated and rhbFGF-treated groups than that of the control group on the seventh day ($^{*}p <$ 0.05). This result indicated that SISAM@HN affected the

https://doi.org/10.1021/acsomega.3c05682
ACS Omega 2023, 8, 46653−46662

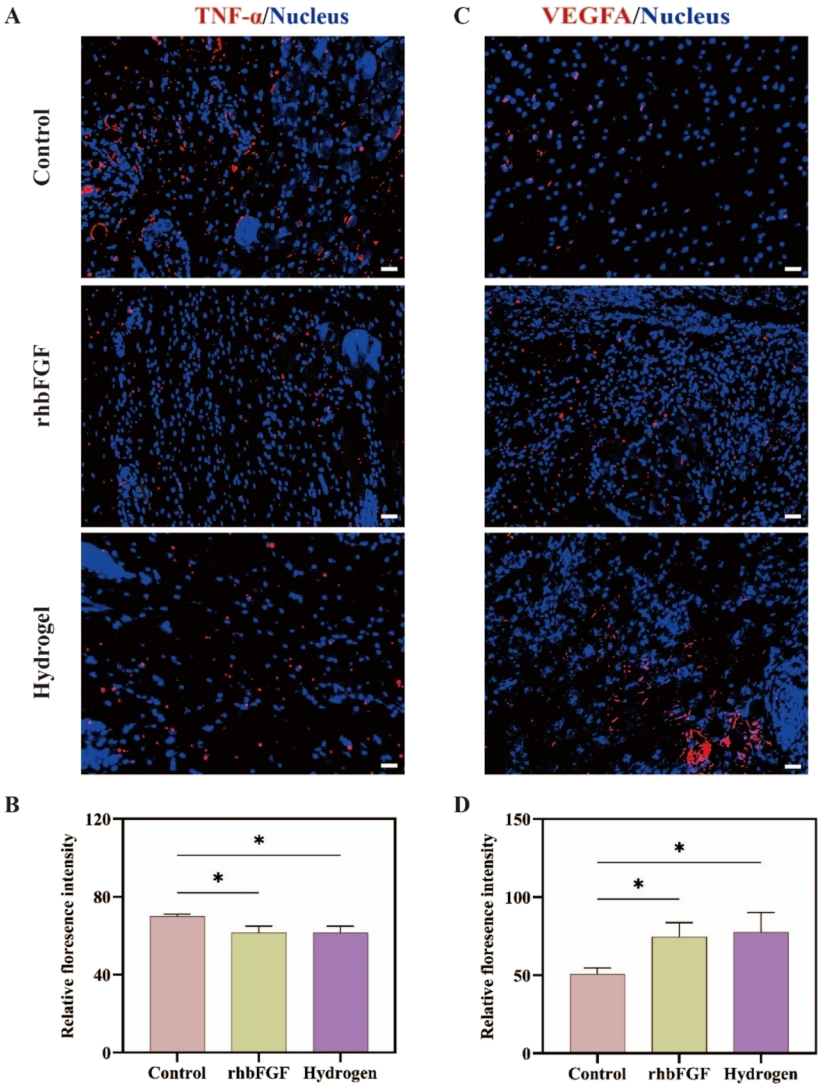

Figure 6. Immunofluorescence staining of tissue sections. (A) Representative immunofluorescence staining images of TNF-α in the wound tissue of the control group, rhbFGF group, and hydrogel group on the seventh day after operation. Scale bar: 100 μm. (B) Statistical analysis of the average fluorescence intensity of positive TNF-α on the seventh day after operation (n = 5, *p < 0.05). (C) Representative immunofluorescence staining images of VEGFA in the wound tissue of the control group, rhbFGF group, and hydrogel group on the seventh day after operation. Scale bar: 100 μm. (D) Statistical analysis of the average fluorescence intensity of positive VEGFA on the seventh day after operation (n = 5, *p < 0.05).

expression of TNF-α and shortened the inflammatory phase.[47] In addition, the expression of VEGF is highly related to angiogenesis and re-epithelization during the wound healing process.[48] Results in Figure 6C,D showed that the SISAM@HN-treated group and rhbFGF-treated group exhibited a higher expression level of VEGFA (red spots) than the control group (**p < 0.01), indicating that the SISAM@HN hydrogel could promote angiogenesis in the wound healing process.[49]

4. CONCLUSIONS

In summary, we designed a composite hydrogel (SISAM@HN) with tissue adhesive properties and bioactive factors for accelerating diabetic wound healing. HA was modified with NB for the phototriggering tissue adhesive capacity, and SISAM contained bioactive factors beneficial to diabetic wound healing. The burst pressure test demonstrated that the *in situ* formed hydrogel possessed a tissue adhesive property. *In vitro* experiments revealed that the SIS acellular matrix-containing hydrogel was able to promote cell proliferation. *In vivo* results showed that the synthesized hydrogel could enhance collagen deposition, attenuate inflammation, and promote vascular growth during the wound healing process in diabetic mice. Overall, the SIS acellular matrix-containing HA hydrogel was able to adhere to the wound sites, promote cell proliferation, and facilitate angiogenesis, which would be a promising biomaterial for wound dressing in clinical therapy of diabetic skin defects.

■ ASSOCIATED CONTENT

Data Availability Statement

All materials are from commercial sources and are widely available. Original data are available from corresponding authors: zjewwei@zju.edu.cn. This paper does not report the original code. Any additional information required to reanalyze the data reported in this paper is available from the lead contact upon request.

https://doi.org/10.1021/acsomega.3c05682
ACS Omega 2023, 8, 46653−46662

AUTHOR INFORMATION

Corresponding Authors

Wei Wei − *Department of Orthopaedic Surgery, the Fourth Affiliated Hospital, International Institutes of Medicine, Zhejiang University School of Medicine, Yiwu, Zhejiang 322000, China; Key Laboratory of Tissue Engineering and Regenerative Medicine of Zhejiang Province, Zhejiang University School of Medicine, Hangzhou, Zhejiang 310000, China;* orcid.org/0000-0002-2234-4459; Email: zjewwei@zju.edu.cn

Kun Zhao − *Department of Endocrinology, the Seventh Medical Center of Chinese PLA General Hospital, Beijing 100700, China*; Email: dr.zhaokun@hotmail.com

Chong Teng − *Department of Orthopaedic Surgery, the Fourth Affiliated Hospital, International Institutes of Medicine, Zhejiang University School of Medicine, Yiwu, Zhejiang 322000, China;* orcid.org/0009-0008-7850-669X; Email: tengchong1984@zju.edu.cn

Authors

Yao Chen − *Department of Orthopaedic Surgery, the Fourth Affiliated Hospital, International Institutes of Medicine, Zhejiang University School of Medicine, Yiwu, Zhejiang 322000, China*

Miner Hu − *Department of Cardiology, the Fourth Affiliated Hospital, International Institutes of Medicine, Zhejiang University School of Medicine, Yiwu, Zhejiang 322000, China*

Honghua Hu − *Department of Orthopaedic Surgery, the Fourth Affiliated Hospital, International Institutes of Medicine, Zhejiang University School of Medicine, Yiwu, Zhejiang 322000, China*

Shunxian Ji − *Department of Orthopaedic Surgery, the Fourth Affiliated Hospital, International Institutes of Medicine, Zhejiang University School of Medicine, Yiwu, Zhejiang 322000, China*

Leyi Huang − *Department of Orthopaedic Surgery, the Fourth Affiliated Hospital, International Institutes of Medicine, Zhejiang University School of Medicine, Yiwu, Zhejiang 322000, China*

Complete contact information is available at: https://pubs.acs.org/10.1021/acsomega.3c05682

Author Contributions

⊥Y.C., M.H., and H.H. contributed equally to this work.

Author Contributions

Y.C., M.H., and H.H. performed investigation and writing of the original draft; Y.C. and L.H. performed animal operation; M.H. performed materials fabrication; H.H. and S.J. performed histological analysis; K.Z., C.T., and W.W. performemd project administration, conceptualization, supervision, and funding acquisition.

Notes

The authors declare no competing financial interest.

ACKNOWLEDGMENTS

This work was supported by the Natural Science Foundation of China (82100843), the Zhejiang Medical and Health Science and Technology Project (2022493383), the Science and Technology program of Jinhua Science and Technology Bureau (Grant No. 2022-3-046), and the Key R&D Program of Zhejiang Province (2023C03076). We thank Hangzhou Shines Biotechnology Co., Ltd for the support of SIS preparation.

REFERENCES

(1) Tu, C.; Lu, H.; Zhou, T.; Zhang, W.; Deng, L.; Cao, W.; Yang, Z.; Wang, Z.; Wu, X.; Ding, J.; Xu, F.; Gao, C. Promoting the healing of infected diabetic wound by an anti-bacterial and nano-enzyme-containing hydrogel with inflammation-suppressing, ROS-scavenging, oxygen and nitric oxide-generating properties. *Biomaterials* **2022**, *286*, No. 121597.

(2) Theocharidis, G.; Yuk, H.; Roh, H.; Wang, L.; Mezghani, I.; Wu, J.; Kafanas, A.; Contreras, M.; Sumpio, B.; Li, Z.; Wang, E.; Chen, L.; Guo, C. F.; Jayaswal, N.; Katopodi, X. L.; Kalavros, N.; Nabzdyk, C. S.; Vlachos, I. S.; Veves, A.; Zhao, X. A strain-programmed patch for the healing of diabetic wounds. *Nat. Biomed. Eng.* **2022**, *6*, 1118−1133.

(3) Xuan, Q.; Jiang, F.; Dong, H.; Zhang, W.; Zhang, F.; Ma, T.; Zhuang, J.; Yu, J.; Wang, Y.; Shen, H.; Chen, C.; Wang, P. Bioinspired intrinsic versatile hydrogel fabricated by amyloidal toxin aimulant-based nanofibrous assemblies for accelerated diabetic wound healing. *Adv. Funct. Mater.* **2021**, *31*, 2106705.

(4) Xu, Z.; Han, S.; Gu, Z.; Wu, J. Advances and impact of antioxidant hydrogel in chronic wound healing. *Adv. Healthcare Mater.* **2020**, *9* (5), No. e1901502.

(5) Fan, L.; Xiao, C.; Guan, P.; Zou, Y.; Wen, H.; Liu, C.; Luo, Y.; Tan, G.; Wang, Q.; Li, Y.; Yu, P.; Zhou, L.; Ning, C. Extracellular matrix-based conductive interpenetrating network hydrogels with enhanced neurovascular regeneration properties for diabetic wounds repair. *Adv. Healthcare Mater.* **2022**, *11* (1), No. e2101556.

(6) Hu, H.; Zhai, X.; Li, W.; Ji, S.; Dong, W.; Chen, W.; Wei, W.; Lu, Z. A photo-triggering double cross-linked adhesive, antibacterial, and biocompatible hydrogel for wound healing. *iScience* **2022**, *25* (7), No. 104619.

(7) Kouhbananinejad, S. M.; Derakhshani, A.; Vahidi, R.; Dabiri, S.; Fatemi, A.; Armin, F.; Farsinejad, A. A fibrinous and allogeneic fibroblast-enriched membrane as a biocompatible material can improve diabetic wound healing. *Biomater. Sci.* **2019**, *7* (5), 1949−1961.

(8) Zhang, Y.; Luo, J.; Zhang, Q.; Deng, T. Growth factors, as biological macromolecules in bioactivity enhancing of electrospun wound dressings for diabetic wound healing: A review. *Int. J. Biol. Macromol.* **2021**, *193* (Pt A), 205−218.

(9) Zhao, X.; Pei, D.; Yang, Y.; Xu, K.; Yu, J.; Zhang, Y.; Zhang, Q.; He, G.; Zhang, Y.; Li, A.; Cheng, Y.; Chen, X. Green tea derivative driven smart hydrogels with desired functions for chronic diabetic wound treatment. *Adv. Funct. Mater.* **2021**, *31* (18), 2009442.

(10) Liang, Y.; He, J.; Guo, B. Functional hydrogels as wound dressing to enhance wound healing. *ACS Nano* **2021**, *15* (8), 12687−12722.

(11) Qi, X.; Tong, X.; You, S.; Mao, R.; Cai, E.; Pan, W.; Zhang, C.; Hu, R.; Shen, J. Mild hyperthermia-assisted ROS scavenging hydrogels achieve diabetic wound healing. *ACS Macro Lett.* **2022**, *11* (7), 861−867.

(12) Yan, L.; Han, K.; Pang, B.; Jin, H.; Zhao, X.; Xu, X.; Jiang, C.; Cui, N.; Lu, T.; Shi, J. Surfactin-reinforced gelatin methacrylate hydrogel accelerates diabetic wound healing by regulating the macrophage polarization and promoting angiogenesis. *Chem. Eng. J.* **2021**, *414*, No. 128836.

(13) Zhang, Y.; Chen, M.; Tian, J.; Gu, P.; Cao, H.; Fan, X.; Zhang, W. In situ bone regeneration enabled by a biodegradable hybrid double-network hydrogel. *Biomater. Sci.* **2019**, *7* (8), 3266−3276.

(14) Hong, H.; Seo, Y. B.; Kim, D. Y.; Lee, J. S.; Lee, Y. J.; Lee, H.; Ajiteru, O.; Sultan, M. T.; Lee, O. J.; Kim, S. H.; Park, C. H. Digital light processing 3D printed silk fibroin hydrogel for cartilage tissue engineering. *Biomaterials* **2020**, *232*, No. 119679.

(15) Schuurmans, C. C. L.; Mihajlovic, M.; Hiemstra, C.; Ito, K.; Hennink, W. E.; Vermonden, T. Hyaluronic acid and chondroitin sulfate (meth)acrylate-based hydrogels for tissue engineering: Syn-

https://doi.org/10.1021/acsomega.3c05682
ACS Omega 2023, 8, 46653−46662

thesis, characteristics and pre-clinical evaluation. *Biomaterials* **2021**, *268*, No. 120602.
(16) Buwalda, S. J.; Boere, K. W.; Dijkstra, P. J.; Feijen, J.; Vermonden, T.; Hennink, W. E. Hydrogels in a historical perspective: from simple networks to smart materials. *J. Controlled Release* **2014**, *190*, 254−73.
(17) Hosseini, M.; Shafiee, A. Engineering bioactive scaffolds for skin regeneration. *Small* **2021**, No. e2101384.
(18) Atashgah, R. B.; Ghasemi, A.; Raoufi, M.; Abdollahifar, M. A.; Zanganeh, S.; Nejadnik, H.; Abdollahi, A.; Sharifi, S.; Lea, B.; Cuerva, M.; Akbarzadeh, M.; Alvarez-Lorenzo, C.; Ostad, S. N.; Theus, A. S.; LaRock, D. L.; LaRock, C. N.; Serpooshan, V.; Sarrafi, R.; Lee, K. B.; Vali, H.; Schonherr, H.; Gould, L.; Taboada, P.; Mahmoudi, M. Restoring endogenous repair mechanisms to heal chronic wounds with a multifunctional wound dressing. *Mol. Pharmaceutics* **2021**, *18* (8), 3171−3180.
(19) Zhou, F.; Hong, Y.; Liang, R.; Zhang, X.; Liao, Y.; Jiang, D.; Zhang, J.; Sheng, Z.; Xie, C.; Peng, Z.; Zhuang, X.; Bunpetch, V.; Zou, Y.; Huang, W.; Zhang, Q.; Alakpa, E. V.; Zhang, S.; Ouyang, H. Rapid printing of bio-inspired 3D tissue constructs for skin regeneration. *Biomaterials* **2020**, *258*, No. 120287.
(20) Widjaja, L. K.; Bora, M.; Chan, P. N.; Lipik, V.; Wong, T. T.; Venkatraman, S. S. Hyaluronic acid-based nanocomposite hydrogels for ocular drug delivery applications. *J. Biomed. Mater. Res., Part A* **2014**, *102* (9), 3056−65.
(21) Yoo, H. S.; Lee, E. A.; Yoon, J. J.; Park, T. G. Hyaluronic acid modified biodegradable scaffolds for cartilage tissue engineering. *Biomaterials* **2005**, *26* (14), 1925−33.
(22) Li, S.; Pei, M.; Wan, T.; Yang, H.; Gu, S.; Tao, Y.; Liu, X.; Zhou, Y.; Xu, W.; Xiao, P. Self-healing hyaluronic acid hydrogels based on dynamic Schiff base linkages as biomaterials. *Carbohydr. Polym.* **2020**, *250*, No. 116922.
(23) Zhao, Y.; Yi, B.; Hu, J.; Zhang, D.; Li, G.; Lu, Y.; Zhou, Q. Double cross-linked biomimetic hyaluronic acid-based hydrogels with thermo-stimulated self-contraction and tissue adhesiveness for accelerating post-wound closure and wound healing. *Adv. Funct. Mater.* **2023**, *33* (26), 2300710.
(24) Lei, T.; Zhao, Y.; Zhai, X.; Ji, S.; Song, B.; Dong, W.; Teng, C.; Wei, W. Photocurable hydrogel-elastomer hybrids as an adhesive patch for meniscus repair. *Mater. Des.* **2023**, *229*, No. 111915.
(25) Yang, Y.; Zhang, J.; Liu, Z.; Lin, Q.; Liu, X.; Bao, C.; Wang, Y.; Zhu, L. Tissue-integratable and biocompatible photogelation by the imine crosslinking reaction. *Adv. Mater.* **2016**, *28* (14), 2724−30.
(26) Zhang, Y.; Li, C.; Zhu, Q.; Liang, R.; Xie, C.; Zhang, S.; Hong, Y.; Ouyang, H. A long-term retaining molecular coating for corneal regeneration. *Bioact. Mater.* **2021**, *6* (12), 4447−4454.
(27) Winkler, J.; Abisoye-Ogunniyan, A.; Metcalf, K. J.; Werb, Z. Concepts of extracellular matrix remodelling in tumour progression and metastasis. *Nat. Commun.* **2020**, *11* (1), 5120.
(28) Wang, K.; Dong, R.; Tang, J.; Li, H.; Dang, J.; Zhang, Z.; Yu, Z.; Guo, B.; Yi, C. Exosomes laden self-healing injectable hydrogel enhances diabetic wound healing via regulating macrophage polarization to accelerate angiogenesis. *Chem. Eng. J.* **2022**, *430*, No. 132664.
(29) Zhang, Y.; Li, M.; Wang, Y.; Han, F.; Shen, K.; Luo, L.; Li, Y.; Jia, Y.; Zhang, J.; Cai, W.; Wang, K.; Zhao, M.; Wang, J.; Gao, X.; Tian, C.; Guo, B.; Hu, D. Exosome/metformin-loaded self-healing conductive hydrogel rescues microvascular dysfunction and promotes chronic diabetic wound healing by inhibiting mitochondrial fission. *Bioact. Mater.* **2023**, *26*, 323−336.
(30) Cao, G.; Huang, Y.; Li, K.; Fan, Y.; Xie, H.; Li, X. Small intestinal submucosa: superiority, limitations and solutions, and its potential to address bottlenecks in tissue repair. *J. Mater. Chem. B* **2019**, *7* (33), 5038−5055.
(31) Wang, M.; Li, Y. Q.; Cao, J.; Gong, M.; Zhang, Y.; Chen, X.; Tian, M. X.; Xie, H. Q. Accelerating effects of genipin-crosslinked small intestinal submucosa for defected gastric mucosa repair. *J. Mater. Chem. B* **2017**, *5* (34), 7059−7071.
(32) Hussey, G. S.; Keane, T. J.; Badylak, S. F. The extracellular matrix of the gastrointestinal tract: a regenerative medicine platform. *Nat. Rev. Gastroenterol. Hepatol.* **2017**, *14* (9), 540−552.
(33) Zhang, X. Z.; Jiang, Y. L.; Hu, J. G.; Zhao, L. M.; Chen, Q. Z.; Liang, Y.; Zhang, Y.; Lei, X. X.; Wang, R.; Lei, Y.; Zhang, Q. Y.; Li-Ling, J.; Xie, H. Q. Procyanidins-crosslinked small intestine submucosa: A bladder patch promotes smooth muscle regeneration and bladder function restoration in a rabbit model. *Bioact. Mater.* **2021**, *6* (6), 1827−1838.
(34) Chen, X. Y.; Wang, Y.; Ma, S. Q.; Huang, Y. Q.; Jing, W.; Wei, P. F.; Yu, X. Q.; Zhao, B. Mechanically active small intestinal submucosa hydrogel for accelerating chronic wound healing. *J. Mater. Chem. B* **2022**, *10* (33), 6279−6286.
(35) Shirzaei Sani, E.; Kheirkhah, A.; Rana, D.; Sun, Z.; Foulsham, W.; Sheikhi, A.; Khademhosseini, A.; Dana, R.; Annabi, N. Sutureless repair of corneal injuries using naturally derived bioadhesive hydrogels. *Sci. Adv.* **2019**, *5* (3), No. eaav1281.
(36) Wei, W.; Ma, Y.; Zhang, X.; Zhou, W.; Wu, H.; Zhang, J.; Lin, J.; Tang, C.; Liao, Y.; Li, C.; Wang, X.; Yao, X.; Koh, Y. W.; Huang, W.; Ouyang, H. Biomimetic joint paint for efficient cartilage repair by simultaneously regulating cartilage degeneration and regeneration in pigs. *ACS Appl. Mater. Interfaces* **2021**, *13* (46), 54801−54816.
(37) Zhu, H.; Luo, H.; Lin, M.; Li, Y.; Chen, A.; He, H.; Sheng, F.; Wu, J. Methacrylated gelatin shape-memorable cryogel subcutaneously delivers EPCs and aFGF for improved pressure ulcer repair in diabetic rat model. *Inter. J. Bio. Macromol.* **2022**, *199*, 69−76.
(38) Wang, Z.; Fu, R.; Han, X.; Wen, D.; Wu, Y.; Li, S.; Gu, Z. Shrinking fabrication of a glucose-responsive glucagon microneedle patch. *Adv. Sci.* **2022**, *9*, 2203274.
(39) Wang, L.; Liu, F.; Zhai, X.; Dong, W.; Wei, W.; Hu, Z. An adhesive gelatin-coated small intestinal submucosa composite hydrogel dressing aids wound healing. *Int. J. Biol. Macromol.* **2023**, *241*, No. 124622.
(40) Yang, Y.; Liang, Y.; Chen, J.; Duan, X.; Guo, B. Mussel-inspired adhesive antioxidant antibacterial hemostatic composite hydrogel wound dressing via photo-polymerization for infected skin wound healing. *Bioact. Mater.* **2022**, *8*, 341−354.
(41) Huang, B.; Hu, D.; Dong, A.; Tian, J.; Zhang, W. Highly antibacterial and adhesive hyaluronic acid hydrogel for wound repair. *Biomacromolecules* **2022**, *23* (11), 4766−4777.
(42) Liu, S.; Zhang, Q.; Yu, J.; Shao, N.; Lu, H.; Guo, J.; Qiu, X.; Zhou, D.; Huang, Y. Absorbable thioether grafted hyaluronic acid nanofibrous hydrogel for synergistic modulation of inflammation microenvironment to accelerate chronic diabetic wound healing. *Adv. Healthcare Mater.* **2020**, *9* (11), No. e2000198.
(43) Wang, Z.; Gao, S.; Zhang, W.; Gong, H.; Xu, K.; Luo, C.; Zhi, W.; Chen, X.; Li, J.; Weng, J. Polyvinyl alcohol/chitosan composite hydrogels with sustained release of traditional Tibetan medicine for promoting chronic diabetic wound healing. *Biomater. Sci.* **2021**, *9* (10), 3821−3829.
(44) Liang, Y.; Li, M.; Yang, Y.; Qiao, L.; Xu, H.; Guo, B. pH/Glucose dual responsive metformin release hydrogel dressings with adhesion and self-healing via dual-dynamic bonding for athletic diabetic foot wound healing. *ACS Nano* **2022**, *16* (2), 3194−3207.
(45) Liu, H.; Li, Z.; Zhao, Y.; Feng, Y.; Zvyagin, A. V.; Wang, J.; Yang, X.; Yang, B.; Lin, Q. Novel diabetic foot wound dressing based on multifunctional hydrogels with extensive temperature-tolerant, durable, adhesive, and intrinsic antibacterial properties. *ACS Appl. Mater. Interfaces* **2021**, *13* (23), 26770−26781.
(46) Annabi, N.; Zhang, Y. N.; Assmann, A.; Sani, E. S.; Cheng, G.; Lassaletta, A. D.; Vegh, A.; Dehghani, B.; Ruiz-Esparza, G. U.; Wang, X.; Gangadharan, S.; Weiss, A. S.; Khademhosseini, A. Engineering a highly elastic human protein-based sealant for surgical applications. *Sci. Transl. Med.* **2017**, *9*, No. eaai7466.
(47) Yuan, Y.; Shen, S.; Fan, D. A physicochemical double cross-linked multifunctional hydrogel for dynamic burn wound healing: shape adaptability, injectable self-healing property and enhanced adhesion. *Biomaterials* **2021**, *276*, No. 120838.

https://doi.org/10.1021/acsomega.3c05682
ACS Omega 2023, 8, 46653−46662

(48) Gao, S.; Zhang, W.; Zhai, X.; Zhao, X.; Wang, J.; Weng, J.; Li, J.; Chen, X. An antibacterial and proangiogenic double-layer drug-loaded microneedle patch for accelerating diabetic wound healing. *Biomater. Sci.* **2023**, *11* (2), 533−541.
(49) Li, Y.; Fu, R.; Duan, Z.; Zhu, C.; Fan, D. Artificial nonenzymatic antioxidant MXene nanosheet-anchored injectable hydrogel as a mild photothermal-controlled oxygen release platform for diabetic wound healing. *ACS Nano* **2022**, *16* (5), 7486−7502.

https://doi.org/10.1021/acsomega.3c05682
ACS Omega 2023, 8, 46653−46662